Identifying controllable and uncontrollable dynamical behavior in complex networks

Jordan C. Rozum
Department of Physics, The Pennsylvania State University
University Park, Pennsylvania, 16802-6300, USA.

Réka Albert
Departments of Physics and Biology, The Pennsylvania State University,
University Park, Pennsylvania, 16802-6300, USA.

March 26, 2018

Abstract

We present a technique applicable in any dynamical framework to identify control-robust subsets of an interacting system. These robust subsystems, which we call stable modules, are characterized by constraints on the variables that make up the subsystem. They are robust in the sense that if the defining constraints are satisfied at a given time, they remain satisfied for all later times, regardless of what happens in the rest of the system, and can only be broken if the constrained variables are externally manipulated. We identify stable modules as graph structures in an expanded network*, which represents causal links between variable constraints. A stable module represents a system "decision point", or trap subspace. Using the expanded network, small stable modules can be composed sequentially to form larger stable modules that describe dynamics on the system level. Collections of large, mutually exclusive stable modules describe the system's repertoire of long-term behaviors. We implement this technique in a broad class of dynamical systems and illustrate its practical utility via examples and algorithmic analysis of two published biological network models. In the segment polarity gene network of* Drosophila melanogaster*, we obtain a state-space visualization that reproduces by novel means the four possible cell fates and predicts the outcome of cell transplant experiments. In the T-cell signaling network, we identify six signaling elements that determine the high-signal response and show that control of an element connected to them cannot disrupt this response.*

A key goal in the study of complex dynamical systems is to extract important qualitative information from models of varying specificity (e.g., [4, 20]). This has been approached via the construction and analysis of qualitative models (e.g., discrete models [1, 29, 31, 13, 23]) and also by analytic techniques applied to continuous systems [25, 26, 2, 5, 19, 22]. In this work, we present and implement a new approach to identifying control-robust subsystem behavior that applies to a large class of continuous, discontinuous, and discrete models. Such behaviors can drive the dynamics of the system as a whole and inform control strategies.

Interacting systems are partially described by their regulatory networks. In these networks, nodes represent each of the various interacting entities within the system, and signed edges represent direct positive or negative influence. To better understand the temporal character of the system, one can construct a dynamical model on the regulatory network. First order ODEs are a natural choice for such models. The influence upon the value of each entity, x_i, is determined according to $\dot{x}_i = F_i(\boldsymbol{x})$, where the dependence of F_i upon x_j is consistent with the influence of entity j upon entity i. A validated model can be used to gain practical insights about the system, such as how to drive it into a desired attractor.

There are two key challenges to the application of these ideas to complex interacting systems. First, there is often large uncertainty in measurements of variable and parameter values. Second, these systems are typically high-dimensional, which complicates phase-portrait visualization and other traditional qualitative analyses. One approach to these challenges is to choose a more qualitative model. Discrete models have been used to successfully model many biological phenomena, including pattern formation and multistability [1, 29]. Another approach is to examine features in the dynamical repertoire that arise directly from the associated regulatory network and weak assumptions about the form of the dynamic model.

Structural controllability relates branching patterns in the regulatory network to the identification of control targets that are sufficient to drive linear dynamics on the network into any state [14]. This allows one to study system control near a steady state. In many biological and chemical systems, however, the dynamics are nonlinear and large disruptions from equilibrium are of interest. In such systems, even when the dynamics are not specifically known, regulatory feedback loops provide useful information for global control [18, 24, 37, 36, 27].

For example, given relatively permissive continuity and boundedness assumptions, an ODE-described system can be driven into any of its attractors by controlling any set of variables whose removal eliminates all feedback loops and external inputs [6, 18, 37]. Positive feedback loops in particular are associated with the presence of multistability [25, 26, 2, 5, 19], which has been of particular interest in biomolecular systems because it is necessary for cell-fate branching and decision making [21, 8, 16, 29, 34].

Two existing approaches to identifying the effects of positive feedback loops are especially relevant here. The first of these is the methods put forth by Angeli and Sontag for studying monotone input-output systems (MIOS) [3]. Their approach identifies steady states and their stability in systems lacking negative feedback loops or incoherent feed-forward loops. The second is based on the concept of *stable motifs* of Boolean dynamical systems [36, 35]. This method constructs an auxiliary network that encodes the regulatory logic within its graph structure, enabling efficient identification of the system's dynamical repertoire. The work presented here can be viewed as an extension of this Boolean methodology that is applicable in any dynamical framework (see Supplemental Material section 1 or [35, 31] for further details).

Our framework encodes the causal relationships between variable constraints as the network structure of an *expanded network*. An edge from one constraint (e.g., $x > 0$) to another (e.g., $y > 0$) indicates that the first ($x > 0$) is sufficient to maintain the second ($y > 0$). The expanded network helps to identify low-dimensional subsystems that drive higher-dimensional dynamics. We show that *stable modules*, source-free expanded subnetworks subject to certain consistency criteria, correspond to self-sustained behavior in the originating dynamical system. Variables obeying stable module constraints must be directly controlled if the constraints are to be broken. This identifies variables that must be controlled to disrupt certain behaviors (or, equivalently, it identifies variables that cannot be controlled in such a way as to disrupt the behavior).

It is non-trivial to choose relevant variable constraints for the modeled system, but in practice, the form of the regulatory functions often suggests natural candidates. Furthermore, we leverage MIOS techniques to algorithmically specify meaningful constraints in a class of systems common in biology (see Supplemental Material section 2). This is implemented (Supplemental Material python source code) as code that systematically scans for stable modules in an input ODE system satisfying certain assumptions. Identifying several stable modules in a systematic search highlights "decision points" in subsystems that determine system-wide outcomes.

Results

Stable Modules Describe Control-Robust Behavior

The core of our analysis strategy lies in the interpretation of an auxiliary network that is constructed from the dynamical system of interest. Following previous work in Boolean systems [1, 30], we call this auxiliary network an *expanded network*. In an expanded network, there are two types of nodes: virtual and composite. Virtual nodes are statements about the values of dynamic variables that can be assigned a definite truth value at any given time (e.g., the virtual node "$x > 0$" is true only when the value of the variable x is positive). Composite nodes also take Boolean values, and correspond to the composition of virtual nodes by "AND" ($\wedge$) rules. Each composite node receives directed edges from its factor virtual nodes. As such, all factors of a composite node must be represented as virtual nodes in the expanded network. For example, the composite node $x > 0 \wedge y > 0$ is true only when x and y are positive, and there are directed edges from $x > 0$ and $y > 0$ to this composite node. In deterministic finite-level systems, it is possible to choose a finite number of statements that fully characterize the state space [33], but in general, the nodes of an expanded network embody partial information about the system.

If a virtual or composite node X must be false *before* a virtual node Y can change from true to false, we say that X *maintains* Y and we draw a directed edge from X to Y in the expanded network. In determining whether X maintains Y, we must consider all valid variable values that might disrupt Y when X is true. These values define a state-space region of validity that may not be fully accessible except when external control is applied. To explore causal relationships among system elements, one may also require that an edge from X to Y indicates that the truth of X implies the truth of Y in finite time; this additional constraint is unnecessary when considering self-sustaining behavior.

A subnetwork, S, of an expanded network, N, is a *stable module* if it satisfies three conditions: (i) all nodes X in S have a parent (regulator) node in S (possibly X itself if it has a self-loop), (ii) if a composite node $X = \bigwedge_{i=1}^{n} X_i$ is in S, then X_i is also in S for $i = 1..n$, and (iii) it is possible for all nodes in S to be simultaneously true. Our key result is the following: if all nodes in a stable module are simultaneously true (if the stable module is *active*), then they remain true under all state-space configurations in the region of validity.

To show this, consider by way of contradiction an active stable module, S that deactivates. Let $Y \in S$ be a virtual node that becomes false before or concurrently with any other node in S. Because S is source-free, there is $X \in S$ that maintains Y. Thus, X (or one of its factors if it is composite) must become false before Y does, violating the selection criteria and thereby proving the result.

A stable module with no stable submodules is a *stable motif*. Under the condition that a stable module, S, is active, we can simplify the expanded network by removing nodes that contradict S as well as edges to composite nodes from virtual nodes in S. Stable motifs of the modified expanded network are then added to S in the original expanded network. We thus iteratively form larger stable modules, building a sequence of stabilized subsystems that drive system dynamics. Mutually exclusive sequences collectively describe the system's dynamical repertoire.

Our definition of stable motifs encompasses the definitions of stable motifs given in [35] for Boolean systems (see Supplemental Material section 1) and in [33] for multi-level systems. This allows us to generalize many results from discrete modeling to general dynamical systems. In particular, generalizing arguments in [36], we consider system control via expanded network topology. It is often of interest to identify variables that can activate a stable module (which may correspond, e.g., to a healthy cell state). This can be achieved by solving the graph-theoretic problem of identifying stable module *driver nodes*. A module *driver node set* D of module M in an expanded network is a set of virtual nodes D such that the truth of all nodes in D implies the truth of all nodes in M in finite time. Therefore, identification of a driver node set for a stable module prescribes a control strategy to trigger the module behavior. Conversely, if a stable module represents undesired behavior (e.g., a diseased cell state), one might seek to disrupt it. Because stable modules are self-sustaining, control of variables not represented in the undesired module can never achieve this goal. Disruption of a stable module requires direct control of at least one of its represented variables.

To illustrate the method, and some of its utility, we analyze a toy example (Fig. 1, Eq. 1).

$$\begin{aligned} \dot{u} =& \frac{1}{1+z} - u^3 \qquad \dot{w} = y - w/2 \qquad \dot{x} = \frac{w+z}{w+1/2} - x \\ \dot{y} =& \frac{x}{x+1/2} - y \qquad \dot{z} = x f(y) - z \qquad f(y) \geq f_{min} > 0 \end{aligned} \quad (1)$$

Here, we have very limited information about $f(y)$; perhaps it is stochastic or discontinuous. Nevertheless, we see that if x is positive, and greater than $\frac{1}{2}$ in particular, z will eventually become and remain positive. We can therefore conclude that there is an edge from $x > \frac{1}{2}$ to $z > 0$ in the expanded network. Similarly, we see that x will be maintained above $\frac{1}{2}$ if $w > \frac{1}{2}$ and $z > 0$ are both true. We therefore identify a composite node $\left(w > \frac{1}{2}\right) \wedge (z > 0)$ with incoming edges from $w > \frac{1}{2}$ and $z > 0$, and an outgoing edge to $x > \frac{1}{2}$. We continue to identify edges in the expanded network and search for stable modules. Some of the subgraphs of the expanded network that can be generated in this way are depicted in Fig. 1 alongside the traditional network representation

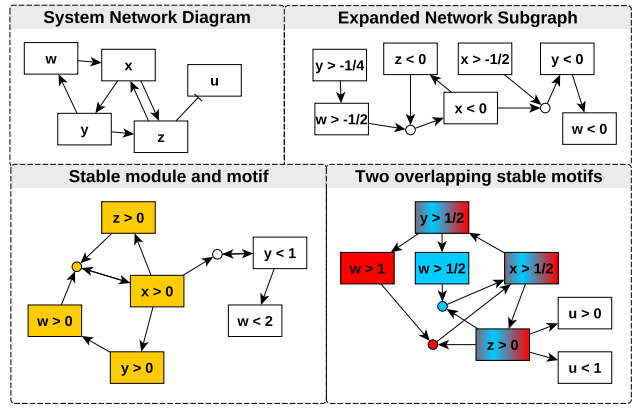

Figure 1: A network representation of the system given in Eq. 1 along with three subgraphs of the expanded network. Each circular node represents a composite node formed by composition of its parent nodes by an "AND" rule. Highlighted components are stable motifs (and therefore also stable modules). These represent conditions that, once satisfied, remain satisfied. In the overlapping motifs (marked in blue and red), we may choose to consider the motif containing $w > 1$ (red), which gives more information about the value of w when the motif is realized, or we may consider the $w > 1/2$ (blue) motif, which is more readily realized. By considering both motifs together, we see that the $w > 1/2$ (blue) motif drives the $w > 1$ (red) motif, i.e., states satisfying $w, x, y > \frac{1}{2}$ and $z > 0$ will eventually also satisfy $w > 1$. We remark also that the stable motifs shown could be expanded to incorporate the other nodes depicted in the components. Such structures are stable modules and are also self-sustaining, but include nodes that are not necessarily part of any feedback loop; they are instead driven by feedback elsewhere in the network.

of the system. We have identified three stable modules, thereby proving, for example, that if the systems satisfies $x, y, w, z > 0$ at any time, it will always satisfy those conditions (as follows from the yellow module in the bottom left of Fig. 1). The other two modules contain $x, y > \frac{1}{2}$ and $z > 0$ as well as either $w > 1$ or $w > \frac{1}{2}$. Thus, if the system satisfies the four conditions given by either module, it will continue to do so for all time. The arguments underlying the construction of the subgraphs of the expanded network hold for any $f(y) > f_{min} > 0$, and so we have extracted meaningful qualitative information despite large dynamical uncertainty. In addition to the subgraphs containing stable modules, many subgraphs that do not contain stable modules also exist. Such subgraphs contain information regarding the consequences of directly controlling particular nodes so that they satisfy virtual node statements (e.g., if we fix $y < 0$, we see that w will eventually become negative).

Choosing virtual nodes defined by inequalities, as is our main focus here, has important implications for how oscillations are observed. If a variable oscillates, but remains above or below some threshold, the statement indicating the variable value relative to that threshold can be part of a stable module. Alternatively, oscillations can manifest

in the expanded network as subnetworks with contradictory virtual nodes.

The main difficulty in identifying stable modules is determining what statements are most useful for inclusion in the expanded network. If the statements are too general, then either the results will not provide much insight, or the network will be too sparse because the statements are not sufficiently restrictive to imply one another. If a statement is too restrictive, on the other hand, it may have an in-degree of zero in the expanded network, in which case it cannot be part of a stable motif. Despite these challenges, we have found a straightforward approach to analyzing threshold behavior of a large class of biologically relevant systems.

Application to Biological Systems

We consider a broad class of dynamical systems that take the form

$$\tau_i \dot{x}_i = F_i\left(\boldsymbol{x}\right), \tag{2}$$

where F_i is continuous, monotonic in each of its arguments, and strictly decreasing in x_i. This class of ODEs describes many biological systems (Supplemental Material section 2) and is particularly well-suited to analysis in our framework (see Supplemental Material section 3 for an example).

To each variable x_i, we assign a set of intervals $\{T_i^\alpha\}$ where T_i^α is of the form $(\inf x_i, a_i)$ or $(b_i, \sup x_i)$. At this stage, each T_i^α may remain parameterized and cover less than the full dynamical range of x_i. We consider virtual nodes $x_i \in T_i^\alpha$ and create composite nodes $\bigwedge_{k=1}^m \left(x_{i_k} \in T_{i_k}^{\alpha_k}\right)$ as needed. Next, we conjecture that particular edges exist in the expanded network for some (unspecified) choice of threshold parameters. For instance, when activity of one variable, x_1, is sufficient for activation of another, x_2, we would hypothesize the formation of an edge $x_1 \in (a, \sup x_1) \rightarrow x_2 \in (b, \sup x_2)$. In the conjectured expanded network, we find candidate stable modules.

What remains is to choose bounds for the virtual nodes to ensure that the candidate stable modules are genuine. We address this by adapting the monotone input-output systems (MIOS) methods of Angeli and Sontag [3]. Following Sontag [24], these techniques are applicable to systems in which we can assign $\sigma_i = \pm 1$ to each node of the associated regulatory network such that the product $\sigma_i \sigma_j$ is 1 whenever nodes i and j are connected by a positive edge, and -1 whenever they are connected by a negative edge. Such networks are called *sign-consistent* networks, and represent systems for which any effect of one variable on another is unambiguously monotonic, implying a lack of negative feedback loops and incoherent feed-forward loops.

By identifying candidate stable modules, we can often apply these methods even when sign inconsistencies are present in the regulatory network. To do this, we consider a candidate stable module, S_c, in the expanded network along with the regulatory subnetwork consisting of nodes represented in S_c and all incident edges. If edges not represented in S_c are removed, the resulting modified regulatory subnetwork is necessarily sign consistent; nodes represented by virtual nodes of the form $x_i \in (\inf F_i, a_i)$ can be assigned $\sigma_i = -1$ and all others can be assigned $\sigma_i = 1$. This is because the only sources of negative regulation in the modified subsystem arise from nodes of this first type, which always contribute negative edges to the modified regulatory subnetwork in pairs.

To construct the sign-consistent modified subsystem for S_c, any regulation of x_i by x_j not represented in S_c, is held fixed by replacing x_j with a "worst-case" value in F_i. The "worst-case" value is chosen such that x_i is as close as possible to a_i or b_i as determined by the stable module node T_i^α; this is either $x_j \equiv \inf x_j$ or $x_j \equiv \sup x_j$. For example, if x_j negatively regulates x_i and $x_i \in (\inf x_i, a_i)$ is in S_c then we evaluate $F_i\big|_{x_j = \inf x_j}$.

Because the resulting modified subsytem is sign-consistent, we are motivated to apply the MIOS procedure of Angeli and Sontag [3, 24]. To do this, we must verify that we can select a set of variables, $\{x_k\}$, called the "MIOS input variables" that are not directly dependent upon one another and have the property that maintaining each x_k at a constant value drives the system to a single steady state for all initial values of variables not in $\{x_k\}$ [3, 24]. The form of equation 2 implies that a node set in the modified system satisfies these conditions if its members are not directly connected in the network and if their removal makes the modified system acyclic. In the systems we have analyzed, node sets of size one have been sufficient for this purpose.

Once we have verified that a set of MIOS input variables can be chosen, we can follow Angeli and Sontag [3, 24] to find the steady states of the modified subsystem. These steady states determine the thresholds a_i and b_i for each variable in the expanded network of the original system such that S_c is realized as a valid stable module. The entire procedure is illustrated in the Supplemental Material section 3.

We have algorithmically implemented (Supplemental Material python source code) this process by considering intersecting unions of positive feedback loops. For each union, we conjecture two stable modules (in which one set of nodes is "high" and the other is "low", and vice versa). Using user-specified physical system bounds, we construct a "worst case system" for each candidate stable module, as described above, and test the existence of a one-variable MIOS input set. If such a variable can be found, we use it to numerically find the steady states via the MIOS procedure. If any steady states are within the physical system bounds, we return the corresponding stable module.

In the remainder of this paper, we use the above methodology and automation scheme to analyze two systems from the literature. The first, the Drosophila segment polarity gene network, is a prototypical system used

to study a broad class of embryonic pattern formation mechanisms. The second example is the T-cell signaling network, which is a characteristic representative of signal transduction networks, which lead to specific cell responses to environmental signals.

Single-Cell Drosophila Segment Polarity Network

The original multicellular model of the Drosophila segment polarity gene network [7] uses coupled ODEs to model the concentrations of mRNAs and proteins of a family of genes that are important for the development of segments in *Drosophila melanogaster* embryos (see Fig. 2). This family of genes includes engrailed and cubitus interruptus, which encode transcription factors, as well as wingless and hedgehog, whose proteins are secreted and interact with proteins in the neighboring cells [7, 10, 9]. We use a modified version of this model (equations 12-23 in [10]), which has incorporated more recent experimental results (e.g., on the *sloppy-paired* protein) and been recast for a single cell while assuming steady-state values for neighboring cells. Because no measured values of the kinetic parameters in the model are available, and because our purpose here is illustrative, we have simply chosen parameter values from the biologically relevant parameter region (see Supplemental Material section 4).

We identify several stable modules of biological importance in this model. When neighboring cells have high levels of *wingless* protein, we find two stable modules distinguished by differential *sloppy-paired* and *engrailed* expression (red and blue nodes in Fig. 2). For high concentrations of neighboring *hedgehog* protein, we find two stable modules involving the *wingless* sub-network (yellow and purple nodes in Fig. 2).

By shading the nodes in the expanded network according to module membership (as in Fig. 2) we can visually identify regions of state-space that correspond to different attractors of the system. Specifically, these attractors distinguish the four cell-types observed in the development of *Drosophila melanogaster* segments, which we label PC1-PC4 [9, 7] (see Fig. 2). Furthermore, the expanded network highlights the causal chains that link regions of state-space and establish cell fates. By identifying driver node sets for stable modules, we can prescribe control strategies to attain any of the four cell types. For example, drivers of the cell type PC1 (blue module in Fig. 2) are high neighboring *hedgehog* (H_{Nbr}) and low *sloppy-paired* (*sp* or SP).

Furthermore, we can use this information to form hypotheses about the outcome of altering node states. For example, consider a cell transplant experiment in which a cell of a certain type is transplanted to a region in which neighboring cells express *hedgehog* and *wingless* at higher or lower levels relative to the cell's initial neighbors. This has the effect of altering the truth values of the elliptical nodes in Fig. 2, potentially disrupting a stable module and changing the qualitative expression pattern of the cell. Consider a cell of type PC1 (blue module in Fig. 2). If the neighboring *hedgehog* (H_{nbr}) and neighboring *wingless* (E_{nbr}) are reversed in expression level, then we have disrupted the *engrailed-sloppy paired* part of the module by changing the value of E_{nbr}, and *en* and *sp* approach zero and one, respectively. The values of *wingless* (*wi*) and the two configurations of its protein before transplant are consistent with the stable module characterizing cell type PC2 (yellow module in Fig. 2). Therefore, our analysis of the model ([10]) suggests that a qualitative change in cell gene expression from that of the foremost cell of the embryonic segment (PC1, blue module) to that of the second segmental cell (PC2, yellow module) would be observed in such a transplant experiment. Our analysis also identifies the reason for this change: the *engrailed-sloppy paired* feedback loop is not robust to elimination of neighboring *wingless* (E_{nbr}). If such a transition is not experimentally observed after transplantation, it is evidence of additional regulation of *engrailed* and/or *sloppy paired*.

T-Cell Receptor Signaling Network

The second biological example we consider here is a model that describes the cascading activation of transcription factors when T-cell receptors are bound by external molecules [32]. The model was constructed using the *Odefy* MATLAB toolbox ([12]) to transform a preexisting Boolean model of T-cell activation ([11]) into an ODE model $\tau_i \dot{x}_i = F_i(\boldsymbol{x}) - x_i$, where each F_i is a polynomial of Hill functions with $F_i(\boldsymbol{x}) \in [0,1]$.

To simplify the example, we consider the strongly connected core of the system with saturated input signals, though the precise signal strength has little impact on the analysis. The resulting network is depicted in Fig. 3a (left), in which the edges are labeled with the Hill coefficient, n, and disassociation constant, k, of the function $H_i(x_i)$ for the corresponding regulatory effect.

By considering when the activation or inhibition of a given node is sufficient or necessary to cause the activation other nodes, we have identified the cycle $TCRb \rightarrow Fyn \rightarrow PAG \rightarrow Lck \rightarrow ZAP \rightarrow cCbl \rightarrow TCRb$ as a candidate stable motif depicted in Fig. 3a (right). This cycle is a positive feedback loop, but it is embedded in a sign-inconsistent network. As such, before we implement the MIOS approach to determine valid thresholds for the motif, we must address the effects of sign-inconsistent edges ([3]). For instance, in the motif, we expect $TCRb$ and PAG to achieve relatively high values, but there is a inhibitory effect between the two; indeed,

$$\begin{aligned} \tau_{PAG} \frac{dPAG}{dt} &= (1 - H_1(TCRb))(1 - H_2(Fyn)) \\ &\quad + H_2(Fyn) - PAG, \end{aligned} \tag{3}$$

where H_1 and H_2 are Hill functions (of the form $\frac{x^n}{x^n + k^n}$ with $n \in \mathbb{Z}^+$ and $k \in (0,1)$). The inhibitory effect is max-

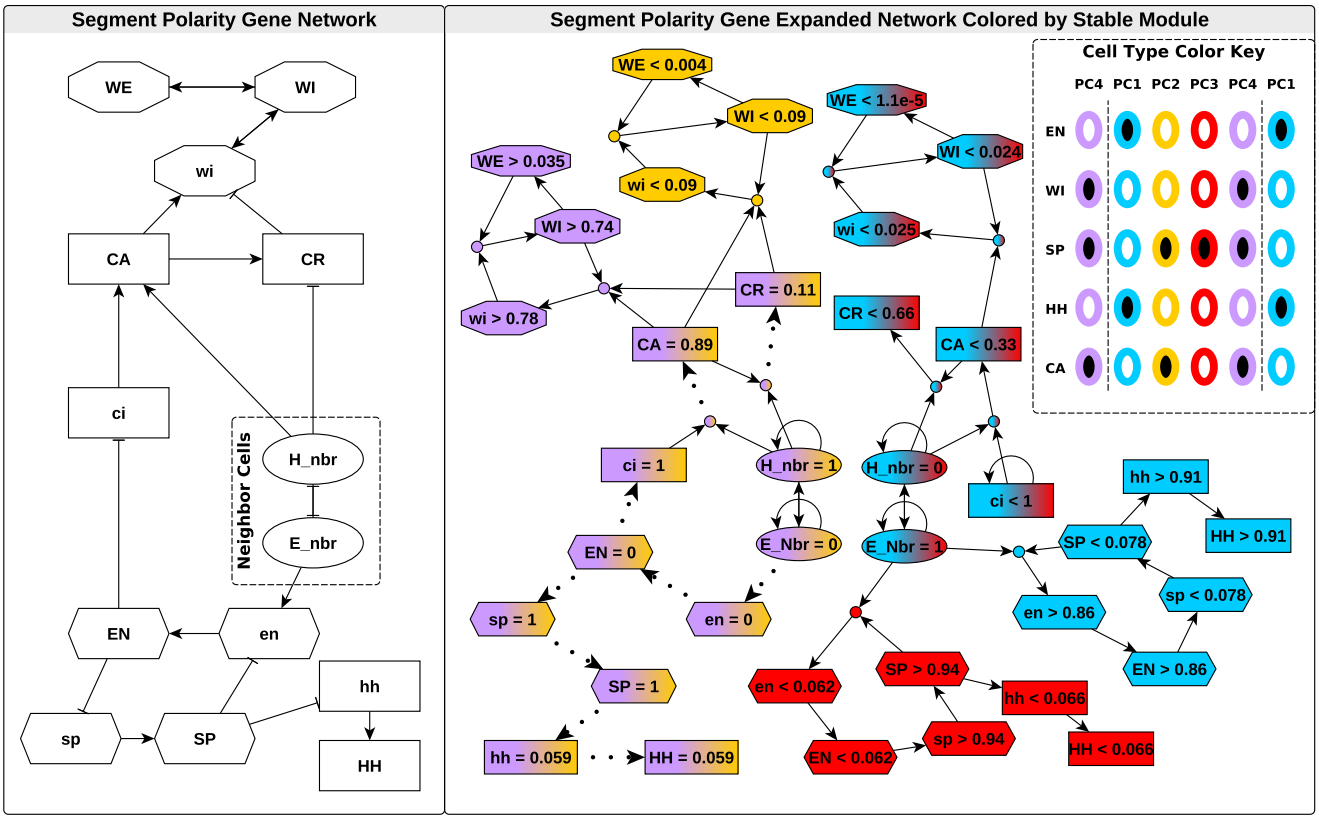

Figure 2: The network schematic for the equations given in [10] (left) and expanded network (right). The color key (right inset) summarizes observed characteristics of cells in the Drosophila *embryonic segments (parasegments) ([7, 10, 9]). Each column represents an individual cell, arranged by anterior-posterior position in the parasegment. Columns are colored and named according to cell type, which is determined by prevalence of the proteins labeling each row. Black-filled ovals represent high levels of the protein, while white-filled ovals represent low levels. In the expanded network (right), dotted lines represent the node maintenance relation and asymptotic implication. Solid lines indicate the maintenance relation and implication in finite time. Nodes are colored according to membership in each of four biologically relevant stable modules, which correspond to the four cell types identified in the right inset. Node shape indicates participation in feedback loops that sustain these stable modules.*

imized when $TCRb$ attains its maximum value, i.e., one (because all variables are normalized to their maximum values in this model). It is also possible to consider the possibility that $TCRb$ is delivered to the system via external control, in which case we would evaluate Eq. 3 in the limit as $TCRb \to \infty$. For now, we shall only consider $TCRb = 1$ in this regulatory function. We therefore replace $H_1(TCRb)$ in Eq. 3 with $H_1(1)$ and allow $TCRb$ to evolve according to its natural dynamics in this new network, in which the regulation of PAG is modified. Similar analysis is taken on any edge that either introduces a sign inconsistency, or does not connect two nodes of the stable motif. The resulting modified network is a single positive feedback loop with a single steady state that is easily identified using the MIOS approach [3]. The steady state values of the nodes in the modified network serve as thresholds in the expanded network, and allow us to identify a stable motif (see Fig. 3a).

We demonstrate the robustness of the stable motif by numerically solving the system ODEs with various constraints placed on $TCRp$ (Fig. 3b). In the top left panel of Fig. 3b, we show a natural evolution of the system for initial conditions satisfying the stable motif conditions. In the other panels, the value of the $TCRp$ node is subjected to one of three external controls (absence, saturation, and oscillation), and the motif variables continue to respect the stable motif conditions. These simulations illustrate an important conclusion we can draw from the existence of the stable motif: If one wishes to avoid states in which Fyn, PAG, and $TCRb$ are high while Lck, ZAP, and $cCbl$ are low, $TCRp$ is not a viable control target. Instead one must disrupt one of the six motif nodes directly, and furthermore, the motif bounds provide lower bounds on the magnitude of the required disruption. For example, to disrupt the motif via control of PAG, one must lower its value below the threshold of 0.69.

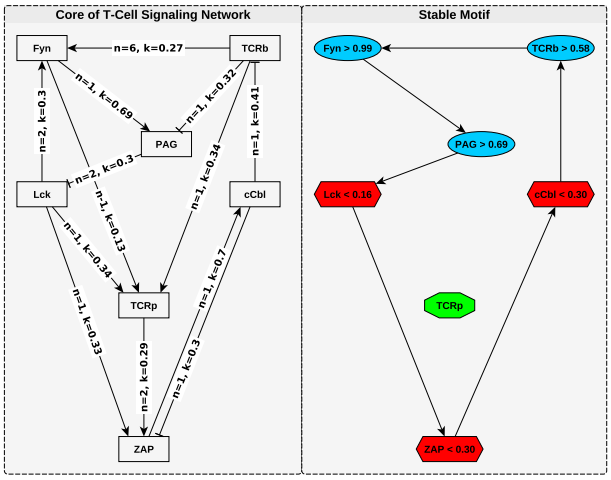

(a)

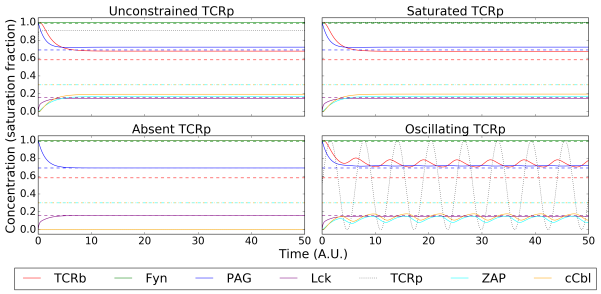

(b)

Figure 3: (a) The network diagram and stable motif for the T-cell signaling model of [32] with all sources saturated. In the stable motif diagram, node shape and color indicate whether an upper or lower bound is specified (as indicated by the node labels). The variables constrained by the stable motif cannot leave the region of state-space specified by the stable motif once it has been entered. This remains true even when $TCRp$, which regulates ZAP, but is not included in the stable motif, is subjected to external control, provided it remains within the bounds considered when constructing the expanded network (between 0 and 1 in this case, though a similar result can be obtained for $0 \leq TCRp < \infty$). This robustness is illustrated in (b), in which solid colored lines indicate dynamic variable values that are constrained by stable motif thresholds (dashed lines). The black dotted line is the $TCRp$ value and is subject to different external controls in panel of sub-figure (b).

Discussion

We have presented a new framework, based upon construction of an auxiliary "expanded network", for identifying self-sustaining subsystems that cannot be controlled via the rest of the system. Full attractor control requires that variables from each of these subsystems be externally manipulated. We have applied our framework to develop an algorithm for finding these subsystems that is applicable in many biological ODE models. We have demonstrated our framework and algorithm in two biological systems: the T-cell receptor signaling network and the *Drosophila melanogaster* segment polarity gene network.

The method of expanded networks can extract important qualitative features from quantitative or qualitative models of system behavior. We have emphasized the identification of stable modules, which correspond state-space regions that, once entered, cannot be exited without directly applying external control on the variables that define the region boundaries. We have also shown, for example in our analysis of the *Drosophila melanogaster* segment polarity gene network, how the consideration of expanded networks can elucidate meaningful and intuitive partitioning of state-space. In these analyses, we have considered virtual nodes of the form $x_i \in (\inf x_i, a_i)$ or $x_i \in (b_i, \sup x_i)$, but other choices for virtual nodes are possible, and can be informative when x_i has inherently multi-level behavior.

Many existing results about the analysis of Boolean models via expanded networks remain valid in this more general framework and can therefore be applied to continuous systems. An example is the concept of a driver node set, which is a set of virtual nodes in the expanded network whose truth eventually implies the truth of a given stable module. Identification of driver nodes in the expanded network is related to finding paths in logic hypergraphs [11]. This identification problem has been partially addressed in [35, 17]; developing a general and fast algorithm for driver node identification in arbitrary expanded networks is a promising direction for future research with applications for control target selection.

Some results do not generalize as easily because they rely upon completeness properties of discrete expanded networks; the oscillation analyses in ([35, 33]) are an example. Oscillations can manifest in the expanded network as source-free graph components that contain contradictory nodes. Such structures do not always indicate oscillatory behavior, and may instead indicate chaotic behavior or the existence of a steady state that violates all of the contradictory conditions. We are optimistic that results of this type might be recast in more general forms.

The expanded network framework shows promise not only for studying the state-space of dynamical systems, as we have emphasized here, but also for the study of parameter space. Statements regarding the value of parameters can be included in an expanded network as statements

with self-loops. Because the expanded network approach extracts qualitative information from the system, the inclusion of parameters in this way is conceptually distinct from and complementary to existing methods for probing the parameter space of a dynamical system (e.g., [28, 15]). The application of expanded networks to parameter sensitivity analyses is the subject of ongoing work.

Acknowledgments

This work was funded by NSF grants PHY 1205840 and PHY 1545832 to RA. We thank Jorge Zañudo for his helpful insights and conversations.

References

[1] Réka Albert and Hans G Othmer. The topology of the regulatory interactions predicts the expression pattern of the segment polarity genes in Drosophila melanogaster. *Journal of Theoretical Biology*, 223(1):1–18, 2003.

[2] David Angeli, James E. Ferrell, and Eduardo D. Sontag. Detection of multistability, bifurcations, and hysteresis in a large class of biological positive-feedback systems. *Proceedings of the National Academy of Sciences*, 101(7):1822–1827, 2004.

[3] David Angeli and Eduardo D. Sontag. Multi-stability in monotone input/output systems. *Systems & Control Letters*, 51(3-4):185–202, 2004.

[4] M. Chaves and M. Preto. Hierarchy of models: From qualitative to quantitative analysis of circadian rhythms in cyanobacteria. *Chaos: An Interdisciplinary Journal of Nonlinear Science*, 23(2):025113, 2013.

[5] G. Craciun and M. Feinberg. Multiple Equilibria in Complex Chemical Reaction Networks: II. The Species-Reaction Graph. *SIAM J. Appl. Math.*, 66(4):1321–1338, January 2006.

[6] Bernold Fiedler, Atsushi Mochizuki, Gen Kurosawa, and Daisuke Saito. Dynamics and control at feedback vertex sets. I: Informative and determining nodes in regulatory networks. *J Dyn Diff Equat*, 25(3):563–604, 2013.

[7] George van Dassow, Eli Meir, Edwin M. Munro, and Garrett M. Odell. The segment polarity network is a robust developmental model. *Nature*, 406, 2000.

[8] Tomáš Helikar, John Konvalina, Jack Heidel, and Jim A. Rogers. Emergent decision-making in biological signal transduction networks. *PNAS*, 105(6):1913–1918, 2008.

[9] Philip W. Ingham. Chapter Twenty-Six - Drosophila Segment Polarity Mutants and the Rediscovery of the Hedgehog Pathway Genes. In Paul M. Wassarman, editor, *Current Topics in Developmental Biology*, volume 116 of *Essays on Developmental Biology, Part A*, pages 477–488. Academic Press, 2016. DOI: 10.1016/bs.ctdb.2016.01.007.

[10] Nicholas T Ingolia. Topology and robustness in the Drosophila segment polarity network. *PLoS Biology*, 2(6):e123, 2004.

[11] Steffen Klamt, Julio Saez-Rodriguez, Jonathan A. Lindquist, Luca Simeoni, and Ernst D. Gilles. A methodology for the structural and functional analysis of signaling and regulatory networks. *BMC Bioinformatics*, 7:56, 2006.

[12] Jan Krumsiek, Sebastian Pölsterl, Dominik M. Wittmann, and Fabian J. Theis. Odefy-from discrete to continuous models. *BMC bioinformatics*, 11(1):233, 2010.

[13] Reinhard Laubenbacher, Franziska Hinkelmann, David Murrugarra, and Alan Veliz-Cuba. Algebraic Models and Their Use in Systems Biology. In *Discrete and Topological Models in Molecular Biology*, Natural Computing Series, pages 443–474. Springer, Berlin, Heidelberg, 2014.

[14] Ching-Tai Lin. Structural controllability. *IEEE Transactions on Automatic Control*, 19(3):201–208, June 1974.

[15] Jason G. Lomnitz and Michael A. Savageau. Elucidating the genotypephenotype map by automatic enumeration and analysis of the phenotypic repertoire. *NPJ systems biology and applications*, 1, 2015.

[16] Javier Macía, Stefanie Widder, and Ricard Solé. Why are cellular switches Boolean? General conditions for multistable genetic circuits. *Journal of Theoretical Biology*, 261(1):126–135, 2009.

[17] Parul Maheshwari and Réka Albert. A framework to find the logic backbone of a biological network. *BMC Systems Biology*, 11:122, 2017.

[18] Atsushi Mochizuki, Bernold Fiedler, Gen Kurosawa, and Daisuke Saito. Dynamics and control at feedback vertex sets. II: A faithful monitor to determine the diversity of molecular activities in regulatory networks. *Journal of Theoretical Biology*, 335:130–146, 2013.

[19] Élisabeth Remy, Paul Ruet, and Denis Thieffry. Graphic requirements for multistability and attractive cycles in a Boolean dynamical framework. *Advances in Applied Mathematics*, 41(3):335–350, 2008.

[20] Raina Robeva and David Murrugarra. The spruce budworm and forest: a qualitative comparison of ODE and Boolean models. *Letters in Biomathematics*, 3(1):75–92, 2016.

[21] M. Santillán, M.C. Mackey, and E.S. Zeron. Origin of bistability in the *lac* operon. *Biophysical Journal*, 92(11):3830–3842, 2007.

[22] Michael A. Savageau, Pedro M. B. M. Coelho, Rick A. Fasani, Dean A. Tolla, Armindo Salvador, and John Ross. Phenotypes and tolerances in the design space of biochemical systems. *Proceedings of the National Academy of Sciences of the United States of America*, 106(16):6435–6440, 2009.

[23] Robert Schwieger and Heike Siebert. Graph Representations of Monotonic Boolean Model Pools. In *Computational Methods in Systems Biology*, Lecture Notes in Computer Science, pages 233–248. Springer, Cham, September 2017.

[24] Eduardo D. Sontag. Monotone and near-monotone biochemical networks. *Systems and Synthetic Biology*, 1(2):59–87, 2007.

[25] R. Thomas and M. Kaufman. Multistationarity, the basis of cell differentiation and memory. I. Structural conditions of multistationarity and other nontrivial behavior. *Chaos*, 11(1):170–179, 2001.

[26] R. Thomas and M. Kaufman. Multistationarity, the basis of cell differentiation and memory. II. Logical analysis of regulatory networks in terms of feedback circuits. *Chaos*, 11(1):180–195, 2001.

[27] Abhinav Tiwari and Oleg A Igoshin. Coupling between feedback loops in autoregulatory networks affects bistability range, open-loop gain and switching times. *Physical Biology*, 9(5):055003, 2012.

[28] Tamás Turányi. Sensitivity analysis of complex kinetic systems. Tools and applications. *J Math Chem*, 5(3):203–248, September 1990.

[29] Alan Veliz-Cuba and Brandilyn Stigler. Boolean models can explain bistability in the *lac* operon. *Journal of Computational Biology*, 18(6):783–794, 2011.

[30] Rui-Sheng Wang and Réka Albert. Elementary signaling modes predict the essentiality of signal transduction network components. *BMC Systems Biology*, 5:44, 2011.

[31] Rui-Sheng Wang, Assieh Saadatpour, and Réka Albert. Boolean modeling in systems biology: an overview of methodology and applications. *Phys. Biol.*, 9(5):055001, 2012.

[32] Dominik M Wittmann, Jan Krumsiek, Julio Saez-Rodriguez, Douglas A Lauffenburger, Steffen Klamt, and Fabian J Theis. Transforming Boolean models to continuous models: methodology and application to T-cell receptor signaling. *BMC Systems Biology*, 3(1):98, 2009.

[33] X. Gan and R. Albert. General method to find the attractors of discrete dynamic models of biological systems. *Phys Rev E (submitted)*, 2017.

[34] G. Yao, C. Tan, M. West, J. R. Nevins, and L. You. Origin of bistability underlying mammalian cell cycle entry. *Molecular Systems Biology*, 7(1):485–485, 2014.

[35] Jorge G. T. Zañudo and Réka Albert. An effective network reduction approach to find the dynamical repertoire of discrete dynamic networks. *Chaos*, 23(2):025111, 2013.

[36] Jorge G. T. Zañudo and Réka Albert. Cell fate reprogramming by control of intracellular network dynamics. *PLOS Computational Biology*, 11(4):e1004193, 2015.

[37] Jorge Gomez Tejeda Zañudo, Gang Yang, and Réka Albert. Structure-based control of complex networks with nonlinear dynamics. *PNAS*, 114(28):7234–7239, 2017.

Supplemental Material

March 25, 2018

1 Boolean Stable Motifs

Here, we expand upon the concepts discussed in [1, 35-37]. A Boolean network is a discrete-time system composed of variables or nodes $X_i(t)$ that can take values in $\{0,1\}$ along with update functions $X_i^*(\{X_i\})$. At each time-step, a subset of $\{X_i(t)\}$ is updated according to $X_i(t+1) = X_i^*(\{X_i(t)\})$. The two most commonly considered update schemes are synchronous update, in which all nodes are updated at each time-step, or general asynchronous update, in which only one randomly selected node is updated at each time-step.

The expanded network of a Boolean system is built by first constructing a pair of virtual nodes for each Boolean variable corresponding to its two states. In a slight abuse of notation, we denote these nodes X_i and $\neg X_i$. To proceed, we note that the Boolean update functions can be written in disjunctive normal form (DNF)

$$X_i^* = \bigvee_{j=1}^{N} \left(\bigwedge_{m=1}^{M_j} X_{l_m} \bigwedge_{q=1}^{Qj} \neg X_{p_q} \right). \tag{1.1}$$

The negation $\neg X_i^*$ of each Boolean function can also be written in DNF. Each term of the form $\bigwedge_{m=1}^{M_j} X_{l_m} \bigwedge_{q=1}^{Qj} \neg X_{p_q}$is called a prime implicant of X_i^* and either corresponds to an existing virtual node, or else we identify the term with a composite node and draw edges from each factor X_{l_m} and $\neg X_{p_q}$ to the composite node. From each node in the expanded network that corresponds to a prime implicant of X_i^* (or $\neg X_i^*$), we draw an edge to the virtual node X_i (or $\neg X_i$). This scheme implies the following: if there is an edge in the expanded network from $\bigwedge_{m=1}^{M_j} X_{l_m} \bigwedge_{q=1}^{Qj} \neg X_{p_q}$ to X_i (or $\neg X_i$), then $\bigwedge_{m=1}^{M_j} X_{l_m} \bigwedge_{q=1}^{Qj} \neg X_{p_q}$ is a term in the DNF of X_i^* (or $\neg X_i^*$). This further implies that whenever $\bigwedge_{m=1}^{M_j} X_{l_m} \bigwedge_{q=1}^{Qj} \neg X_{p_q}$ and X_i are active, X_i will always update to 1 in the next update step. As such, the Boolean expanded network, as described above, is an expanded network of the type described in the main text. It is also noteworthy that the update functions X_i^* can be reconstructed from the expanded network.

A stable motif in the expanded network is a subgraph S with the following properties: (i) all nodes in S have a parent (regulator) in S or else have a self-loop, (ii) S does not include any contradictory nodes, (iii) S includes all the parents (regulators) of included composite nodes, and (iv) S has no proper subgraphs satisfying the first three properties (note that condition (iv) implies that S is strongly connected). We call subgraphs satisfying the first three conditions *stable modules*. Such network components correspond to values of the Boolean variables that are stable, independent of the rest of the system.

As an example, consider the following Boolean network:

$$\begin{aligned} A^* &= A \wedge B \\ B^* &= A \vee C \\ C^* &= A \wedge B \vee \neg C \end{aligned} \tag{1.2}$$

For convenience, we give the negated update functions as well:

$$\begin{aligned} \neg A^* &= \neg A \vee \neg B \\ \neg B^* &= \neg A \wedge \neg C \\ \neg C^* &= (\neg A \wedge C) \vee (\neg B \wedge C). \end{aligned} \tag{1.3}$$

We can now construct the expanded network, as the update rules and their negations are written in DNF in Equations 1.2 and 1.3. By inspecting these rules, as written, we see that in addition to the virtual nodes A, B, C, $\neg A$, $\neg B$, and $\neg C$, we will need to construct composite nodes $A \wedge B$, $\neg A \wedge \neg C$, $\neg A \wedge C$, and $\neg B \wedge C$, for a total of ten nodes. We draw edges to the composite nodes from each of their factors (e.g., there are edges from A and B to $A \wedge B$). We also draw edges to the virtual nodes according to the prime implicants of the update rules (e.g., there are edges from A and C to B, and edges from $\neg A \wedge C$, and $\neg B \wedge C$ to $\neg C$). The completion of this procedure yields the full Boolean expanded network.

We graphically represent the network given by Equations 1.2, construct its expanded network, and identify stable motifs in Figure 1.1. This network has only two attractors. The first is the steady state in which all variables are true. The second is the one in which A is false, and B and C oscillate. The existence and nature of these two attractors, and the absence of other attractors, is independent of the update scheme, although the precise nature of the oscillation in the second attractor does depend upon the update scheme. There are three stable motifs. The first consists of only $\neg A$, and this stable motif captures the behavior that if A ever becomes false, it remains false. The other two stable motifs both contain A, B, and $A \wedge B$. One also contains C. The A, B, and $A \wedge B$ motif indicates that if A and B are both true, they both remain true, independent of C (e.g., if $C = 0$ were held fixed by some external control, $A = B = 1$ would remain stable). The motif that also contains C identifies $A = B = C = 1$ as a steady state of the system.

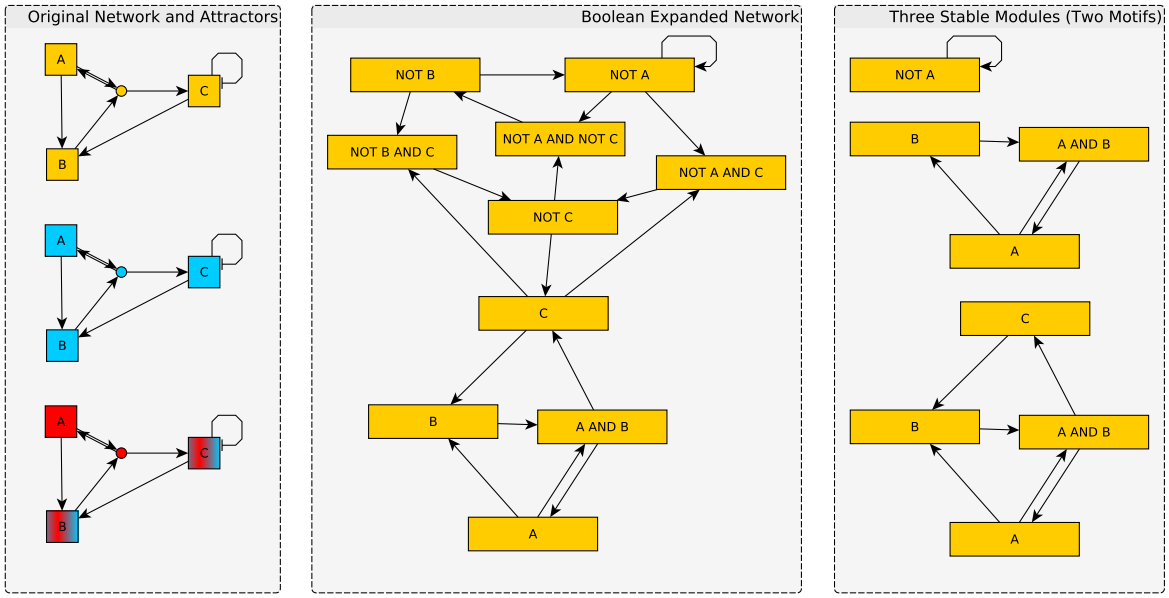

Figure 1.1: From left to right: (i) schematic of the network from Equations 1.2 with its two attractors (blue is true, red is false, and the gradient represents oscillation) (ii) the full expanded network of Equations 1.2 (iii) the three stable modules that exist in the network. The "NOT A" stable module (motif) captures the behavior that if A ever becomes false, it remains false. The other two stable modules identify the steady-state attractor of the system.

2 Dynamical Properties of Biomolecular Systems

The dynamics of biomolecular systems are almost always bounded (i.e. the within-cell concentrations of proteins or molecules do not increase without bound). Furthermore, most biomolecular interactions and regulatory relationships are monotone. In some cases for which this does not hold, the non-monotonic behavior arises from the effect of as-of-yet unknown mediators that form network motifs such as incoherent feed-forward loops, which create ambiguous indirect relationships. For example, in considering the regulatory relationship $\dot{x} = w^3 - w - x$, we might at first believe that w is a non-monotonic regulator of x, when in reality, a more accurate model of the system might be $\dot{x} = y - z - x$, $\dot{y} = \alpha\left(w^3 - y\right)$, $\dot{z} = \alpha\left(w - z\right)$, which does include only monotonic regulatory functions and involves two additional mediators that have opposite effects on x (this example is especially believable when $\alpha \gg 1$, because y and z will respond extremely quickly to changes in w). This situation is likely in biomolecular networks, in which regulatory relationships are often not mapped to the level of elementary reactions and it is infrequent that a regulator such as a transcription factor or enzyme directly inhibits certain processes (transcription or reactions) and activates others.

For these reasons, we focus on ODE systems that take the form

$$\tau_i \dot{x}_i = F_i\left(\boldsymbol{x}\right) - x_i, \tag{2.1}$$

where F_i is continuous, monotonic in each of its arguments, and bounded.

3 Example: Identification of a Stable Module

Consider the system

$$\begin{aligned}
\dot{w} &= H\left(z\right) - w \\
\dot{x} &= H\left(w\right) - x \\
\dot{y} &= H\left(x\right) - y \\
\dot{u} &= x - u \\
\dot{z} &= 1 + H\left(y\right) H\left(u\right) - H\left(u\right) - z \\
H\left(\cdot\right) &= \frac{\left[\cdot\right]^2}{\left[\cdot\right]^2 + 1/4}.
\end{aligned} \tag{3.1}$$

By inspection, we note that the following structure is present in the expanded network, for unspecified thresholds:

$$\left(z > T_z\right) \rightarrow \left(w > T_w\right) \rightarrow \left(x > T_x\right) \rightarrow \left(y > T_y\right). \tag{3.2}$$

We therefore conjecture the existence of a stable module that includes this structure and $\left(y > T_y\right) \rightarrow \left(z > T_z\right)$. The only edge in the regulatory network incident to a variable represented in this candidate motif that is not represented in this candidate motif is the regulation of z by u. This is a negative edge because $H\left(y\right) < 1$, and makes the network sign-inconsistent. To search for valid thresholds for

this candidate motif, we fix the effect of this edge at the "worst case" value. In this example, that corresponds to the value of x that most greatly inhibits z. Because u will be bounded by $\sup x = \sup H(w) = 1$, that value is $u = 1$. This yields the following modified system:

$$\begin{aligned} \dot{w} &= H(z) - w \\ \dot{x} &= H(w) - x \\ \dot{y} &= H(x) - y \\ \dot{z} &= 1 + H(y) H(1) - H(1) - z. \end{aligned} \tag{3.3}$$

Note that this is a monotone, sign-consistent system because we are holding the sign-inconsistent regulation fixed. We now find the steady states of this modified system following the MIOS procedure outlined in [3, 24]. The steady states correspond to the roots of the function feedback function

$$k(z) = 1 + H(H(H(H(z)))) H(1) - H(1) - z, \tag{3.4}$$

which is obtained by considering the regulation of (e.g.,) z by its inputs when the regulatory effect of z (on w) is held fixed (i.e., w will approach $H(z)$, so x will approach $H(H(z))$, and so on until z approaches $k(z) + z$). There are three roots of this equation in the interval $(0, 1)$. We consider the largest root, which we call r and find numerically to be $r = 0.679468149712$, though the following discussion is equally valid with either other root used in place of r. The modified subsystem has a steady state

$$w = x = y = H(r), \; z = r, \tag{3.5}$$

and so $(z > r) \rightarrow (w > H(r)) \rightarrow (x > H(r)) \rightarrow (y > H(r)) \rightarrow (z > r)$ is a stable module (we may, by inspection of the original system, extend the module to include $(x > H(r)) \rightarrow (u > H(r))$).

We interpret this result as follows. If $w, x, y > H(r)$ and $z > r$ hold at any time, then these will continue to hold for all time. This is true even if u is externally controlled, provided u remains smaller than one. If we are unsatisfied with this restriction on u, we may instead take the "worst-case" value for u to be infinity (rather than one), in which case the resulting characteristic has only one root, $1/2$, in $(0, 1)$; this corresponds to the stable motif $\left(z > \frac{1}{2}\right) \rightarrow \left(w > \frac{1}{2}\right) \rightarrow \left(x > \frac{1}{2}\right) \rightarrow \left(y > \frac{1}{2}\right) \rightarrow \left(z > \frac{1}{2}\right)$, which has a similar interpretation.

4 Parameters for the Segment Polarity Model

Using the model and notation of [26], equations (3) and (11)-(23) the parameters we have used in our consideration of the *Drosophila* segment polarity gene regulatory network are as follows:

For all time constants (H): $H = 1$

For all Hill functions (Φ): $K = 0.25$, $\nu = 2$

For all modified regulatory functions (Ψ): $K = 0.5$, $\nu = 4$, $a_0 = 0.1$

For *wingless* diffusion: $C_0 = 0.5$, $K_{in,WG} = K_{out,WG} = 0.05$